

A RESONANT CAVITY METHOD OF MEASURING THE VELOCITY OF LIGHT

Thesis by

Hans Emil Wohlwill

In Partial Fulfillment of the Requirements

For the Degree of

Doctor of Philosophy

California Institute of Technology

Pasadena, California

1954

## ACKNOWLEDGMENTS

The work described herein was carried out under the supervision of Professor W.H. Pickering. The author wishes to express his gratitude to Dr. Pickering for his constant encouragement and for the very fruitful research conferences that guided the progress of this thesis.

Thanks are also due many members of the staff for valuable advice and for their kind cooperation. The author is particularly indebted to the following: Professor R.V. Langmuir of the Electrical Engineering Department; Professors W.A. Fowler, W.R. Smythe, and R.B. Leighton of the Physics Department; Dr. W.A. Wenzel, formerly of the Physics Department; Professor D.M. Yost of the Chemistry Department, Mr. W.W. Schuelke of the Chemistry Instrument Shop; Mr. H.H. Reamer of the Chemical Engineering Department; and Professor P. Kyropoulos of the Mechanical Engineering Department.

## ABSTRACT

A contribution to the precision measurement of the velocity of light is described. The experiment makes use of a circular cylindrical cavity operating in the  $TE_{011}$  mode and resonant in the 3 centimeter region. For a particular length-to-diameter ratio the resonance frequency is only a function of the cavity volume and the velocity of propagation of electromagnetic waves. The latter can be calculated from an experimental determination of resonance frequency and cavity volume.

The object of this experiment was to attain an accuracy of one part in 150,000 for each individual determination. The resonant frequency was measured with a precision of one part in a million; the precision of the volume measurement was one part in 180,000. The corrections applying to both of these measurements can be calculated with sufficient accuracy to correspond to the above figures. Unfortunately, however, a time limit prevented a proper experimental determination of one correction; this concerns the shift in resonant frequency due to the iris coupling between the input wave guide and the cavity. It would be difficult to assign a numerical value to the uncertainty introduced by the lack of this information, but a minimum value for the velocity of light can be obtained.

The experiments led to a probable result of

$$299,809 \text{ km/sec,}$$

measured with a precision of  $\pm 1$  km/sec. The extreme value of the uncertainty in the iris correction corresponds to -19 km/sec, indicating a minimum value of

$$299,790 \text{ km/sec.}$$

This is to be compared to the best two recent determinations whose results are 299,789 km/sec and 299,793 km/sec.

# TABLE OF CONTENTS

| PART |                                    | PAGE |
|------|------------------------------------|------|
| I.   | HISTORICAL SURVEY                  | 1    |
| II.  | THEORY OF THE MEASUREMENT          | 3    |
|      | 1. The Ideal Cavity                | 3    |
|      | 2. Cavity Corrections              | 4    |
|      | 2.1. The Losses                    | 6    |
|      | 2.2. Small Deformations            | 7    |
|      | 2.3. The Coupling Irises           | 7    |
|      | 2.4. The Thin Iris                 | 8    |
|      | 2.5. The Thick Iris                | 17   |
| III. | APPARATUS AND MEASURING TECHNIQUE  | 19   |
|      | 1. The Cavity                      | 19   |
|      | 2. The Frequency Measurement       | 19   |
|      | 3. The Volume Measurement          | 27   |
|      | 4. The Temperature Measurement     | 30   |
| IV.  | THE EXPERIMENTS                    | 32   |
|      | 1. The Frequency Measurement       | 32   |
|      | 2. The Volume Measurement          | 38   |
|      | 3. The Weighings                   | 42   |
|      | 4. Experimental Results            | 43   |
|      | 5. Calculations                    | 47   |
|      | 6. Calibrations                    | 50   |
| V.   | DISCUSSION                         |      |
|      | 1. The Interfering $TM_{111}$ Mode | 51   |
|      | 2. The Input Wave Guide Mismatch   | 52   |
|      | 3. Additional Sources of Error     | 53   |
|      | 4. The Dielectric Constant of Air  | 56   |
|      | 5. Conclusions                     | 57   |
|      | APPENDIX                           | 58   |
|      | REFERENCES                         | 60   |

# LIST OF ILLUSTRATIONS

|  | PAGE |
|--|------|
| Fig. 1. Cavity and Wave Guide Fringe Fields  | 9    |
| Fig. 2. Cavity and Wave Guide Fringe Fields  | 10   |
| Fig. 3. Cavity and Wave Guide Termination  | 13   |
| Fig. 4. Cavity Assembly Drawing  | 20   |
| Fig. 5. Block Diagram of Frequency Measuring Apparatus                               | 21   |
| Fig. 6. Resonance Curve with Frequency Markers                                       | 26   |
| Fig. 7. Apparatus for Filling Cavity   | 28   |
| Fig. 8. Detail of Capillary-Cavity Joint   | 28   |
| Fig. 9. Resonance Curve with Second Harmonics  | 33   |
| Fig. 10. Frequency vs. Temperature, in Vacuo   | 44   |
| Fig. 11. Frequency vs. Temperature, in Vacuo, Calculated<br>from Measurements in Air | 45   |
| Fig. 12. Enlarged Detail of Iris and Capillary                                       | 55   |

## I. HISTORICAL SURVEY

The velocity of light is a fundamental physical constant. A knowledge of its exact value is of great importance because many other physical constants are derivable from it.

During the last few decades, a number of high precision determinations have been made using both optical methods and resonant cavity techniques. In 1926, A.A. Michelson (1) used the rotating mirror method and a path between Mount Wilson and Mount San Antonio near Pasadena, California. He obtained the value  $299,796 \pm 4$  km/sec for the velocity of light in vacuo. This experiment was repeated by a number of investigators who introduced many refinements. In 1941, Birge (2) adopted a weighted average of these results, namely

$$299,776 \pm 4 \text{ km/sec.}$$

During World War II, radar navigation data indicated that the above value was too low by perhaps as much as 20 km/sec. This appears to be confirmed by two very recent measurements resulting in a value near 299,790 km/sec. In one of these, E. Bergstrand (3) used a frequency modulated Kerr cell and phototube and obtained a value of  $299,792.7 \pm 0.25$  km/sec. This represents a remarkably direct measurement requiring very few corrections. The other experiment is one initiated by W.W. Hansen and carried on by K. Bol at Stanford University. A circular cylindrical cavity is used, operating in the  $TE_{012}$  and  $TE_{021}$  modes. The resonant frequencies of these two modes are measured,

eliminating an absolute measurement of the diameter. A provisional result (1950) is given by K. Bol (4) as  $299,789.3 \pm 0.4$  km/sec.

In 1948, the present experiment was started by Dr. H. Gruenberg, then an instructor and graduate student in the Electrical Engineering Department at the California Institute of Technology. This experiment also uses the resonant cavity method. It was his idea to eliminate both length and diameter measurements, and replace them by a volume measurement. A knowledge of the volume to one part in 50,000 corresponds to an accuracy of  $\pm 1$  km/sec in the velocity of light. This method further eliminates the necessity of constructing a cavity with optically true surfaces. Gruenberg's preliminary experiments led to a result of  $299,764 \pm 15$  km/sec (5).

It was the author's task to refine the equipment and experimental procedure in order to reduce the error to the minimum value inherent in the method.

## II. THEORY OF THE MEASUREMENT

### 1. The Ideal Cavity

The cavity is a circular cylinder of diameter  $D$  (or radius  $R$ ), length  $L$ , operating in the  $TE_{011}$  mode. This mode has no wall currents crossing the joints between the cylinder and the end plates; hence a perfect electrical contact is unnecessary. The resonant frequency,  $f$ , of this mode is given by (see, for example, Smythe (6), eqs. 15.11(3) and 15.03(2))

$$\left(\frac{2\pi f}{c}\right)^2 = k^2 + \left(\frac{\pi}{L}\right)^2 \quad (2.1)$$

where

$c$  = propagation velocity of electromagnetic waves

$kR$  = first root of  $J'_0(x) = -J_1(x) = 0$ .

Letting  $L = \rho D$ , (2.1) can be rewritten:

$$c = \frac{f}{(kR)} (4\pi^2 V)^{1/3} \frac{\rho^{2/3}}{[\rho^2 + (\frac{\pi}{kD})^2]^{1/2}} \quad (2.2)$$

where  $V = \frac{1}{4} \pi D^2 L$  is the volume of the cavity. If in (2.2)  $\rho$  is considered a variable, we can find the value  $\rho = \rho_0$  for which  $c$  (or more precisely  $f \cdot \sqrt[3]{V}$ ) is stationary. Differentiating  $[\rho^2 + (\frac{\pi}{kD})^2] \rho^{-4/3}$  with respect to  $\rho$  and setting the derivative equal to zero we obtain

$$\rho_0 = \frac{\pi}{\sqrt{2}} \frac{1}{(kR)} \quad (2.3)$$



For a cavity with such a length-to-diameter ratio (2.2) reduces to

$$c = \frac{f}{\sqrt{3}} \times \sqrt[3]{\frac{16\pi V}{(kR)^2}} . \quad (2.4)$$

Thus, if the required accuracy in the value of  $c$  is 1 part in 150,000, the frequency has to be measured to that accuracy, but the volume need be known to only 1 part in 50,000. Gruenberg (5, p. 11) shows that if the construction or measurement error in  $\rho$  is less than  $\frac{1}{4}$  per cent, its effect on the value of  $c$  can be neglected.

## 2. Cavity Corrections

Following Gruenberg (5, part V), the fields in the cavity are expanded in a series of orthogonal modes:

$$\text{Vector Potential } \check{\underline{A}} = \sum_a \check{\underline{A}}_a = \sum_a \check{p}_a \underline{A}_a^0 . \quad (2.5)$$

If  $\underline{A}_a^0$  is normalized by

$$\int_V \underline{A}_a^0 \cdot \underline{A}_a^0 dV = V \quad (2.6)$$

and if

$$\check{\underline{E}}_a^0 = -j \omega \underline{A}_a^0 \quad (2.7)$$

$$\underline{B}_a^0 = \nabla \times \underline{A}_a^0 , \quad (2.8)$$

then  $\check{\underline{E}}_a^0$  and  $\underline{B}_a^0$  are normalized as follows:

$$\int_V \check{\underline{E}}_a^0 \cdot \check{\underline{E}}_a^0 dV = \omega_a^2 V \quad (2.9)$$

$$\int_V \underline{B}_a^0 \cdot \underline{B}_a^0 dV = \beta_a^2 V , \quad (2.10)$$

where  $\beta = \frac{\omega}{c}$ . The fields  $\check{\underline{A}}$ ,  $\check{\underline{E}}$ , and  $\check{\underline{B}}$  all have the same amplitude coefficients,  $\check{p}_a$ . The ideal cavity fields can now be written:

$$\underline{A}_a^0 = \underline{a}_\Phi \sqrt{2} \frac{J_1(kr)}{J_0(kR)} \sin \frac{\pi z}{L} \quad (2.11)$$

$$\underline{E}_a^0 = -\underline{a}_\Phi j\omega \sqrt{2} \frac{J_1(kr)}{J_0(kR)} \sin \frac{\pi z}{L} \quad (2.12)$$

$$\underline{B}_a^0 = \frac{\sqrt{2}}{J_0(kR)} \left[ -\underline{a}_r \frac{\pi}{L} J_1(kr) \cos \frac{\pi z}{L} + \underline{a}_z k J_0(kr) \sin \frac{\pi z}{L} \right], \quad (2.13)$$

where

$$R = \frac{1}{2} D = \text{radius of cavity.}$$

In particular, we need to know the magnetic field at the iris, i.e.,

at  $r = R$ ,  $z = \frac{1}{2} L$ .

$$\underline{B}_a^0(0) = \underline{a}_z \sqrt{2} k \quad (2.14)$$

or

$$[B_a^0(0)]^2 = 2k^2.$$

From (2.1) and (2.3)

$$k^2 = \frac{2}{3} \beta_a^2.$$

Thus

$$[B_a^0(0)]^2 = \frac{4}{3} \beta_a^2. \quad (2.15)$$

From a simple vector identity involving the ideal field  $\underline{A}_a^0$  and the actual field  $\check{\underline{A}}$ , Gruenberg derives the following important formula:

$$(\beta^2 - \beta_a^2) \check{p}_a = - \frac{1}{j\omega V} \int_s \underline{n} \times \check{\underline{E}} \cdot \underline{B}_a^0 dS. \quad (2.16)$$

This equation not only enables us to calculate the frequency shift due to all perturbations, but gives us a formula for the amplitude of oscillations. The following perturbations are considered:

The losses due to the finite conductivity of the surface material (silver);

Small deformations;

The coupling irises.

## 2.1. The Losses

It is shown (5, pp. 30-32) that the losses introduce a frequency shift

$$\frac{\Delta f}{f} = - \frac{1}{2Q} \quad (2.17)$$

where

$$Q = \frac{30\pi^2 (3)^{3/2}}{R_s (1 + 2\rho_o)} = \frac{713}{R_s} \quad (2.18)$$

and

$R_s$  = skin effect surface resistance.

It is to be emphasized here that (2.17) accounts for the entire effect of the finite conductivity of the cavity surface. In (2.4) the velocity of propagation,  $c$ , depends on the ideal resonant frequency,  $f$ , which is deduced from the measured resonant frequency by applying appropriate corrections such as (2.17); it further depends on  $V$ , which is the actual volume as measured.  $V$  is not an effective volume which is made larger than the measured one by the addition of a shell of thickness equal to the "skin-depth" of the surface material. This question has recently come up in connection with other resonant cavity measurements of  $c$  (14).

In this case  $Q$  in (2.17) is the usual  $Q$  associated with a resonant system; i.e.,  $\frac{1}{Q}$  is the normalized bandwidth of the resonance curve.

## 2.2. Small Deformations

A formula is derived (5, p. 34) which shows that the frequency shift introduced by a boundary deformation is determined by the electric or magnetic fields in the deformation region, being positive for a region of high electric field, negative for one of high magnetic field. It is shown that neither ellipticity in the cavity body nor a tilt in the end plates contribute any frequency shift.\* Similarly, a small taper in the cylindrical surface does not affect the resonant frequency. In addition, the following two formulas represent the effect of small grooves in the cavity surface, of depth  $h$  and width  $b$ .

$$(\text{cylinder}) \quad \frac{\Delta f}{f} \sim - \frac{2}{3} \frac{\pi R b h}{V} \quad (2.19)$$

$$(\text{end plates}) \quad \frac{\Delta f}{f} \sim - \frac{1}{3} \frac{\pi R b h}{V} . \quad (2.20)$$

## 2.3. The Coupling Irises

There are two irises located diametrically opposite on the cylindrical surface, half-way between the end plates (i.e.,  $z = \frac{1}{2} L$ ,  $r = R$ ). A standard 3 centimeter wave guide section is attached to the cavity so that the wave guide magnetic field is in the  $z$  direction, coupling directly to the cavity field (see 2.14). The irises are

---

\* This holds to first order.

actually tapered holes whose larger diameters are on the wave guide sides. To simplify the theory the thin iris will be considered in detail; the case of the thick iris will be treated qualitatively.

#### 2.4. The Thin Iris

The problem is simple in principle. Equation (2.16) can be applied directly. The only unknown quantity on the right hand side is  $\check{E}$ , which is the actual electric field in the hole. This field is associated with that part,  $\check{B}_0$ , of the magnetic field which causes the fringing from the cavity into the wave guide.  $\check{B}_0$  is called the effective exciting field.  $\check{E}$  is calculated approximately from the static field distribution of  $\check{B}_0$  using Smythe's double current sheet method (7). By this method (5, pp. 39-40)  $\check{E}$  is obtained in terms of  $\check{B}_0$  as follows:

$$\underline{n} \times \check{E} = j \frac{2}{\pi} \omega \check{B}_0 (c^2 - \rho^2)^{1/2} \quad (2.21)$$

where

$c$  = radius of iris

and

$\rho$  = radius variable in the iris.

Substituting (2.21) into (2.16) the right hand side becomes

$$-\frac{1}{V} \frac{4}{3} c^3 \check{B}_0 [B_a^0(0)].$$

Letting  $\frac{4}{3} c^3 = M$ , which is called the iris polarizability, (2.16) becomes:

$$(\beta^2 - \beta_a^2) \check{p}_a = -\frac{M}{V} \check{B}_0 [B_a^0(0)]. \quad (2.22)$$

The problem has now been reduced to finding  $\check{\underline{B}}_0$  in terms of  $\underline{B}_a^0(0)$  or  $\check{\underline{B}}_a(0) = \check{p}_a \underline{B}_a^0(0)$ .

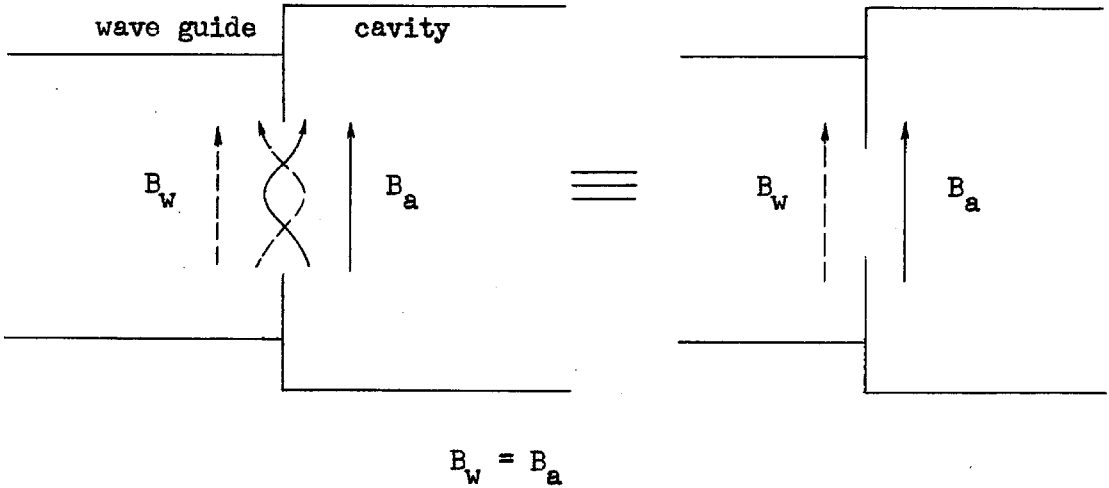


Fig. 1. Cavity and Wave Guide Fringe Fields

A clear understanding must be gained of the effect of the wave guide field on the "effective exciting" field in the cavity. In Fig. 1,  $B_w$  and  $B_a$  denote the magnitude of the unperturbed fields, i.e.,  $B_w$  is the dominant - mode ( $TE_{10}$ ) magnetic field in the wave guide,  $B_a$  is the ideal resonant cavity field ( $TE_{011}$  mode). The illustration shows that if  $B_w = B_a$  the fringe fields cancel: i.e., this case is equivalent to the case of an ideal cavity where the iris is replaced by a perfect conductor. Thus, in this case there would be no frequency shift.

In Fig. 2 is shown how the wave guide field must be taken into account. It shows the superposition of the case of Fig. 1 and the fringe field caused by the effective field  $\check{\underline{B}}_0 = \check{\underline{B}}_a - \check{\underline{B}}_w$ .

It must be noted here that even if the wave guide is matched, i.e., none of the energy radiated from the iris comes back,  $\check{B}_w$  still must be subtracted from  $\check{B}_a$  in order to obtain the field  $\check{B}_o$  which causes the fringing and therefore the frequency shift. In this case,  $\check{B}_w$  is the  $TE_{10}$  mode matched magnetic field. Or again, if the iris were to radiate into free space,  $\check{B}_w$  would be the plane- or spherical-wave field (the propagating field) and would have to be subtracted from  $\check{B}_a$ .

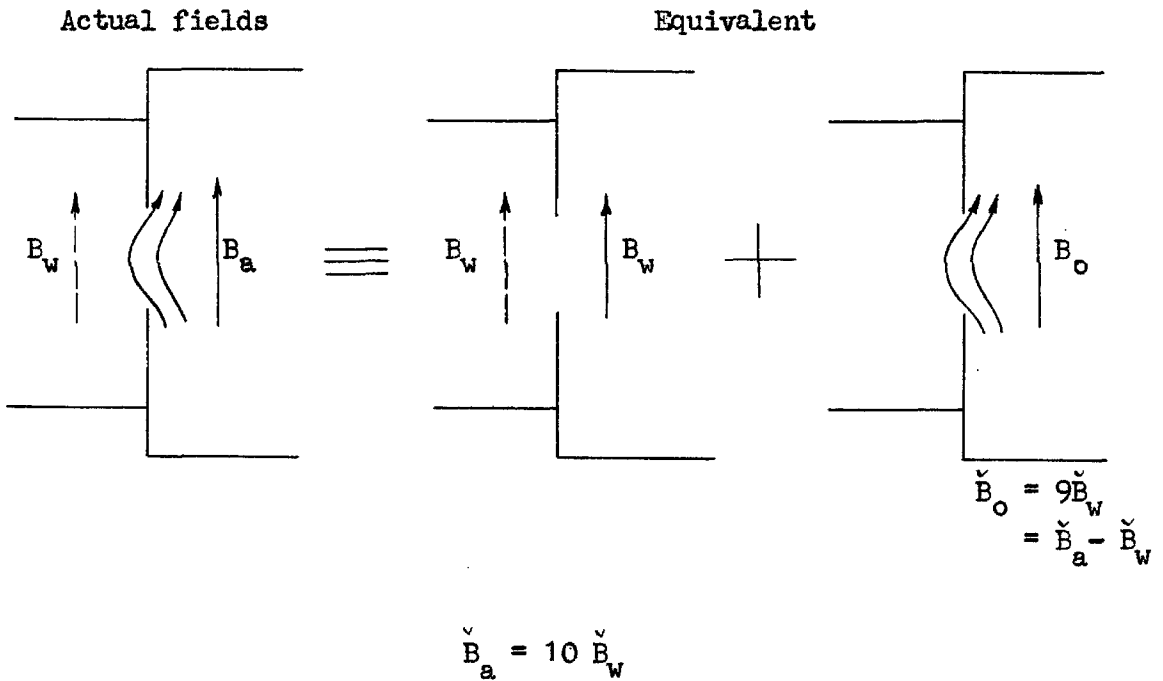


Fig. 2. Cavity and Wave Guide Fringe Fields

### A. Wave Guide Matched

Consider, first, the matched case. This means that the wave guide, looking out from the cavity, is matched so that none of the field radiating from the iris, is reflected back.

The problem is to find the magnetic field,  $\check{\underline{B}}_w$ , which propagates in the wave guide, i.e., the  $TE_{10}$  mode. We know the electric field distribution in the iris from (2.21). When this is matched to the  $TE_{10}$  mode in the guide we obtain

$$\check{\underline{E}}_w = \frac{2j \omega M \check{\underline{B}}_o}{ab},$$

where

$a, b$  = wave guide dimensions.

If the wave guide is perfectly terminated, the corresponding magnetic field is

$$\check{\underline{B}}_w = j \frac{4\pi M}{\lambda_{g ab}} \check{\underline{B}}_o = j \Psi \check{\underline{B}}_o \quad (2.23)$$

where

$\lambda_g$  = guide wave length,

and

$$\Psi = \frac{4\pi M}{\lambda_{g ab}} = 0.008 \text{ numerically.}$$

The exciting field  $\check{\underline{B}}_o = \check{\underline{B}}_a(0) - \check{\underline{B}}_w = \check{\underline{B}}_a(0) - j \Psi \check{\underline{B}}_o$ , so that

$$\check{\underline{B}}_o = \frac{1}{1 + j\Psi} \check{\underline{B}}_a(0). \quad (2.24)$$

For all practical purposes this can be written

$$\check{\underline{B}}_o = (1 - j\Psi) \check{\underline{B}}_a(0). \quad (2.25)$$



The right hand side of (2.22) now becomes

$$\begin{aligned} -\frac{M}{V} (1 - j\Psi) \check{E}_a(0) [E_a^0(0)] &= -\frac{M}{V} (1 - j\Psi) \check{p}_a [B_a(0)]^2 \\ &= -\frac{M}{V} \frac{4}{3} \beta_a^2 (1 - j\Psi) \check{p}_a, \text{ using (2.15).} \end{aligned}$$

Equation (2.22) now reads:

$$[\beta^2 - \beta_a^2 + \frac{4}{3} \frac{M}{V} (1 - j\Psi) \beta_a^2] \check{p}_a = 0, \quad (2.26)$$

where the right hand side should, strictly speaking, be replaced by the forcing function. The following remarks can be made about (2.26)

- (1) The real part of the correction term,  $\frac{4}{3} \frac{M}{V} \beta_a^2$ , is responsible for the frequency shift.
- (2) The imaginary part,  $-\frac{4}{3} \frac{M}{V} \Psi \beta_a^2$ , indicates the losses introduced by the iris, and is thus responsible for a change in  $Q$ . The corresponding  $Q_i$  can be calculated directly from (2.26). It is

$$Q_i = \frac{3}{4} \frac{V}{M\Psi} \quad (2.27)$$

since  $\frac{4}{3} \frac{M}{V} \ll 1$ .

$Q_i$  can also be obtained another way: calculate the power propagated in the wave guide from a knowledge of  $\check{E}_w$  and  $\check{B}_w$ . From this  $Q_i$  can be found readily. The result is identical with (2.27).

## B. Arbitrary Wave Guide Termination

This case differs from the previous case only in that the ratio  $\check{B}_w/\check{E}_w$  will change in magnitude and become complex, i.e.,  $\Psi$  will be multiplied by a complex factor.

The following relations from transmission line theory will be needed. It will be understood that  $K$ ,  $z$ , and  $y$  are complex numbers. The complex number sign ( $\sim$ ) will also be left out when writing  $B$ ,  $B_w$ , etc. Subscripts  $+$  and  $-$  denote waves traveling away from, and towards the cavity, respectively:

$$\text{Reflection coefficient } K = \frac{B_+}{B_-} = \frac{y - 1}{y + 1},$$

where  $z$  and  $y$  are normalized wave guide impedance and admittance, respectively.

$$\text{VSWR} = \frac{1 + |K|}{1 - |K|}$$

(Note: The conventional reflection coefficient is defined as  $-K$ .)

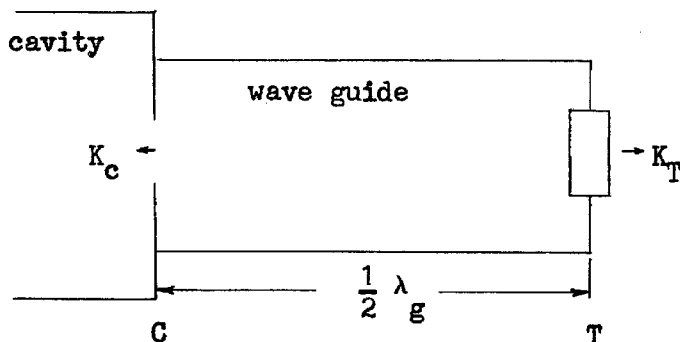


Fig. 3. Cavity and Wave Guide Termination

At the cavity

$$K_c = \frac{-jb_c - 1}{-jb_c + 1} = 1 \angle -\alpha$$

where

$$b_c > 10, \quad \alpha < 10^\circ.$$

In order to take into account the effect of the iris on the wave guide fields, it appears that the simplest approach is to consider the infinitely many reflections and sum them.

The original field radiating from the iris into the wave guide is the same as if the wave guide were matched, i.e., it is from (2.23),  $B_w = j\psi B_o$ . This field reaches point T, a half wave length away, where it is reflected. Thus,

At T:  $B_+ = B_w$ .

The first reflected wave is

$$B_{-1} = K_T B_w$$

At C:  $B_{-1}$  is reflected and becomes

$$B_{+1} = K_c K_T B_w$$

Total field at C becomes

$$B_{-1} + B_{+1} = (1 + K_c) K_T B_w$$

At T:  $B_{-2} = K_c K_T^2 B_w$

At C:  $B_{+2} = K_c^2 K_T^2 B_w$

Total field:  $B_{-2} + B_{+2} = (1 + K_c) K_c K_T^2 B_w$ .

Similarly:

At C: Total field:  $B_{-3} + B_{+3} = (1 + K_c) K_c^2 K_T^3 B_w.$

Adding all fields at C:

$$\begin{aligned} \Sigma (B_{-n} + B_{+n}) &= B_w [1 + (1 + K_c) K_T \sum_{n=0}^{\infty} (K_c K_T)^n] \\ &= B_w \left[ 1 + \frac{(1 + K_c) K_T}{1 - K_c K_T} \right]. \end{aligned}$$

Thus the  $TE_{10}$  mode component of the total magnetic field at C is

$$B_{wt} = B_w \frac{1 + K_T}{1 - K_c K_T}. \quad (2.28)$$

This is the field to be subtracted from the ideal cavity field, i.e., substituting  $j\Psi B_o$  for  $B_w$  we obtain

$$B_{wt} = j\Psi \frac{1 + K_T}{1 - K_c K_T} B_o$$

and, as in (2.24)

$$B_o = \frac{1}{1 + j\Psi \frac{1 + K_T}{1 - K_c K_T}} B_a(0). \quad (2.29)$$

Let

$$\frac{1}{1 + j\Psi \frac{1 + \check{K}_T}{1 - \check{K}_c \check{K}_T}} = \check{f} \quad (2.30)$$

Then (2.29) becomes

$$\check{B}_0 = \check{f} \check{B}_a(0)$$

and (2.26) now reads

$$(\beta^2 - \beta_a^2 + \frac{4}{3} \frac{M}{V} \check{f} \beta_a^2) \check{p}_a = 0. \quad (2.31)$$

A few special cases will be discussed.

Case 1. Wave guide matched.

$$\text{This means } \check{K}_T = 0.$$

$\check{f}$  then reduces to  $(1 + j\psi)^{-1} \approx 1 - j\psi$  and (2.31) is identical with (2.26), as it should be.

Case 2. Wave guide section resonant at resonant frequency of cavity.

$$\text{This means } \check{K}_c \check{K}_T = 1.$$

$$\check{f} \rightarrow 0.$$

This case then introduces no shift in the resonant frequency whatsoever.

Case 3. Termination  $T$  is arbitrary. Neglect phase angle  $\alpha$  of  $\check{K}_c$ .

$$\text{Then } \frac{1 + \check{K}_T}{1 - \check{K}_c \check{K}_T} \approx \frac{1 + \check{K}_T}{1 - \check{K}_T} = \check{y}_T$$

and  $\check{f}$  becomes

$$\check{f} = \frac{1}{1 + j\psi \check{y}_T}.$$

If  $|\check{y}_T| \leq 10$  and  $\check{y}_T = g_T + jb_T$ , we can write

$$\check{f} = 1 + \psi b_T - j\psi g_T. \quad (2.32)$$

Thus, if the termination is inductive the frequency shift is decreased relative to the matched case by the factor  $1 - \Psi|b_T|$ . If it is capacitive, the shift is increased by the factor  $1 + \Psi|b_T|$ .<sup>\*</sup> It is thus easy to determine to what accuracy  $\check{Y}_T$  or  $b_T$  has to be measured for a given allowed tolerance on the frequency correction. If, for instance, the frequency correction for each iris has to be known within 7 per cent, the effect of mismatch can be neglected completely if  $|b_T| \leq 8$ . Or again, if  $|b_T| \sim 100$ ,  $b_T$  has to be measured with 15 per cent accuracy.

## 2.5. Thick Iris

In the case of the thick iris, including that of a tapered hole, the preceding arguments and formulas still hold. Only  $\Psi$  may become complex, and its absolute value will be reduced for two reasons:

1. The electric field which excites the  $TE_{10}$  mode in the wave guide is less than that on the cavity side of the iris by the amount of attenuation in the iris itself. This reduces  $\check{E}_w$  relative to  $\check{E}_0$  and therefore  $\check{B}_w$  relative to  $\check{B}_0$  (2.23).

2. When calculating the effective exciting field  $\check{B}_0$ , only some fraction of the field  $\check{B}_{wt}$  (i.e., the  $TE_{10}$  mode field on the wave guide

---

<sup>\*</sup> This result can perhaps be understood by an electric circuit analogy. The coupling network between the primary resonant circuit (the cavity) and the output network (the wave guide) is such that for a small change in an output parameter the input to the coupling network changes from the antiresonant (parallel resonance, i.e., high impedance) to the resonant condition (series resonance, i.e., low impedance). For antiresonance the primary resonance frequency will not be shifted. For series resonance the primary frequency will be shifted a relatively large amount. In the matched case there will be some loading which shifts the resonance frequency an intermediate amount.

side of the iris) should be subtracted from  $\check{B}_a(0)$ , this fraction corresponding to the attenuation in the iris looking towards the cavity. This again only affects the value of  $\Psi$  as seen by the derivation of (2.24).

In addition, of course, the value of  $M$  is reduced by the factor  $A_1\pi$  (5, eq. (5.61)) due to the change in the electrostatic field distribution.

If we modify the value of  $\Psi$  as explained above and let the new value be  $\check{\Psi}'$ , then we can write (cf. (2.32))

$$\check{f} = 1 + (\text{Re } \check{\Psi}') b_T + (\text{Im } \check{\Psi}') g_T + j[(\text{Im } \check{\Psi}') b_T - (\text{Re } \check{\Psi}') g_T] \quad (2.33)$$

The frequency correction will be given by

$$\Delta f = [1 + (\text{Re } \check{\Psi}') b_T + (\text{Im } \check{\Psi}') g_T] \Delta f_0$$

where  $\Delta f_0$  is the value of the correction for the matched case.

Thus  $\check{\Psi}'$  can be determined experimentally if  $\Delta f$  is measured for various values of  $b_T$  and  $g_T$ .

Similarly, using the imaginary term, the unloaded cavity  $Q$  can be calculated from loaded  $Q$  measurements.

The preceding considerations apply, of course, to both input and output irises.

### III. APPARATUS AND MEASURING TECHNIQUE

#### 1. The Cavity

The cavity with its wave guide flanges is shown in Fig. 4. The cavity body itself was constructed with comparatively heavy flanges to make it as strong as possible. It was made of cold-rolled steel and silver plated, the plating thickness (0.0002 inches) being an order of magnitude larger than the skin depth for silver at the operating frequency ( $\sim 10^{10}$  cycles). The actual mean cavity dimensions, as measured, were

$$D = 1.9797 \text{ inches}$$

$$L = 1.1479 \text{ inches}$$

with maximum variations of  $\pm 0.0005$  inch.

From the above numbers we obtain

$$\rho_o = \frac{L}{D} = 0.57983,$$

compared to the theoretical

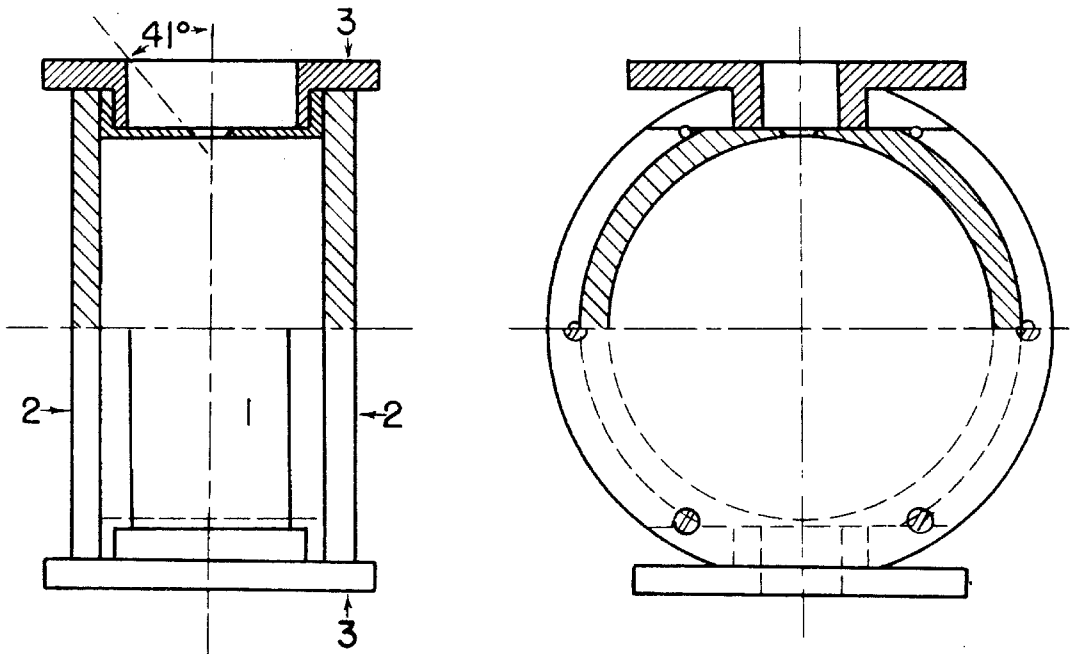
$$\rho_o = \frac{\pi}{\sqrt{2} \text{ (kR)}} = 0.57975.$$

This represents an error in  $\rho_o$  of  $+0.00014$ , insignificant compared to the allowable error of  $1/4$  per cent.

#### 2. Frequency Measurement

A microwave generator, frequency modulated by a 5 cycle sine wave, supplies power to the cavity (see Fig. 5). The power transmitted through the cavity is detected by a silicon crystal, amplified, and fed





- 1. MAIN BODY
- 2. END PLATES
- 3. WAVE GUIDE FLANGES

FIGURE 4-CAVITY ASSEMBLY DRAWING, FULL SCALE

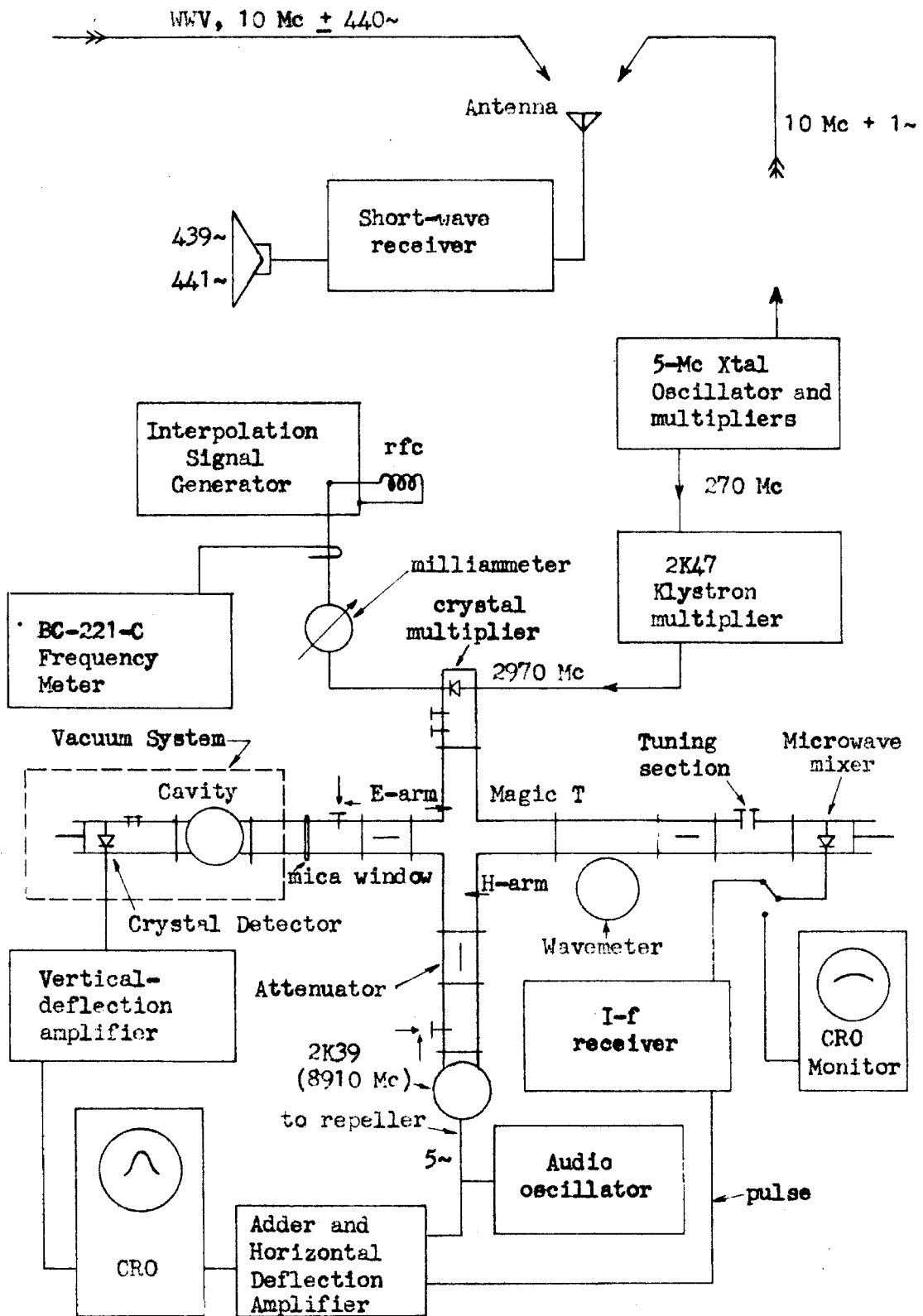


Fig. 5. Block Diagram of Frequency Measuring Apparatus.

to the vertical deflection terminals of a cathode-ray oscilloscope. The resonance curve of the cavity is thereby displayed on the screen of the oscilloscope. The microwave generator also serves as the local oscillator in a superheterodyne receiver. Its signal is combined with one or two of several frequency standard signals in a microwave mixer. The frequency standard signals are obtained by subtracting the output of a radio-frequency signal generator (about 2 megacycles) from a fixed standard (8910.0000 megacycles) which is a harmonic of a 5 megacycle quartz crystal oscillator. The mixer output is fed to a receiver which passes signals only when the local oscillator frequency differs from the "standard" frequency by an amount equal to the receiver setting within a range of about 10 kilocycles. The frequency markers produced in this manner are amplified and added to the 5 cycle modulation signal to be displayed on the oscilloscope as horizontal pips. There are a number of ways of using these pips, but the method essentially amounts to adjusting the variable frequency standard until its frequency coincides exactly with that of the top of the cavity resonance curve. Coincidence is judged by the horizontal alignment of two pips. This is most easily illustrated as follows. If the cavity resonance is at  $f_0$ , which is also the setting of the frequency standard, and if the receiver is tuned to  $\Delta f$ , then the receiver will respond at two points in the local oscillator modulation cycle, given by  $f_0 \pm \Delta f$ . Since the resonance curve is symmetric\* the cavity response will be the same at these two points, accounting for the horizontal alignment of the frequency markers.

---

\* Experimentally some asymmetry was found to exist. See part V.

The secondary frequency standard consisted of a 5 megacycle crystal oscillator and a chain of frequency multipliers. The crystal temperature was thermostatically controlled. A condenser in parallel with the crystal made possible slight adjustments in the crystal frequency, so it could be set exactly to 5 megacycles by comparison with standard frequency broadcasts from radio station WWV near Washington, D.C. It was possible to set the crystal frequency to 5 megacycles within about  $1/16$ th of a cycle, as follows: the two audio notes produced by heterodyning the crystal signal with the two audio side bands of the WWV signal interfere with each other to produce an audio note whose intensity is modulated at a low rate, say, once every four seconds.\* One cannot carry this process too far, however, for if the intensity modulation becomes too slow it is difficult to distinguish from the natural fading of the WWV signal. Moreover, since  $1/16$ th cycle at 5 megacycles is one part in  $10^8$  one has already gone slightly beyond the guaranteed stability of the WWV signal received in California.

Conventional class-C triplers and one doubler were used to bring the frequency up to 90 megacycles. Two 6C4 miniature triodes were used to drive a type 832A beam power tube in push-pull to amplify the 90 megacycle signal. The output was used to drive the final tripler stage which also made use of a type 832A tube operating in push-pull. A power output of approximately 4 watts was available at 270 megacycles.

This power was used to drive a type 2K47 Sperry klystron, which is a velocity modulation frequency multiplier. The output cavity was tuned to the eleventh harmonic, or 2970 megacycles.

---

\* The method described multiplies the carrier frequency error by 2. The error is multiplied by another factor of 2 by using the second harmonic of the crystal and receiving WWV at 10 megacycles. Thus an intensity modulation at  $1/4$  cycle corresponds to an error of  $1/16$ th cycle at 5 megacycles.

This frequency was tripled again in a 1N21 silicon crystal mounted across a standard 3 centimeter wave guide. The output from the 2K47 was sufficient to produce a d-c crystal current of 5 to 10 milliamperes. The signal strength at the 8910 megacycle level was high enough to be read on a microammeter connected to the mixer crystal. The 1N21 tripler was also used to mix the output of the radio-frequency signal generator with the 8910 megacycle signal. A number of "standard" frequencies, are thus produced, all propagating in the wave guide. Those of primary interest are the 8910 megacycle signal and that given by  $8910 - f_s$ , where  $f_s$  is the setting of the signal generator.

A type 2K39 reflex klystron was used as the main power source, and as the local oscillator. It was tuned to about 8910 megacycles and frequency modulated by coupling a 5 cycle signal to the repeller through a condenser. It is necessary to provide cooling for the klystron. When using forced air for this purpose it was found that the air produced strong enough vibrations in the tuning diaphragm to make the klystron frequency unstable over a range of about 100 kilocycles. When the klystron was immersed in an oil bath (transformer oil proved quite satisfactory) this trouble disappeared completely.

The local oscillator and standard frequency signals were combined in a magic T in such a way as to avoid coupling between them. The two signals were mixed in a 1N23 crystal whose output (the difference frequency) was fed to a receiver as described above.

The cavity was mounted in an evacuated bell jar. A vacuum-tight joint in the wave guide system was provided by a commercial mica

window mounted in a flange suitable for a 3 centimeter wave guide. The flange was machined flat in order to effect an "O-ring" seal with a standard "choke"-flange, which is provided with an O-ring groove.

The power transmitted through the cavity was detected in a 1N23B crystal which was selected for maximum sensitivity. The output section was carefully adjusted by means of two tuning screws and a movable shorting plunger to provide a good match as seen from the cavity. The detected signal was fed to the vertical-deflection amplifier through a shielded cable. The amplifier was designed to have a phase shift of less than  $1^{\circ}$  from 5 cycles to 5,000 cycles.

The receiver was U.S. Navy communications equipment. Its intermediate-frequency response was modified to pass a band of about 10 kilocycles. The output was taken from the detector stage and added to the modulation signal to provide the horizontal input to the oscilloscope. The adder stage also was designed for negligible phase shift. The circuit employed a double triode with a common cathode resistor. That section connected to the receiver output was a cathode follower biased to cut-off. The receiver pulse causes additional cathode current to flow which appears as a pulse at the output terminals of the second section.

The system produced a picture on the screen of the oscilloscope similar to that shown in Fig. 6. The presence of four pulses instead of two is due to the use of a full sine wave instead of a saw-tooth wave for frequency modulation. It is seen that this method essentially eliminates the effects of all phase shifts in the entire system, including

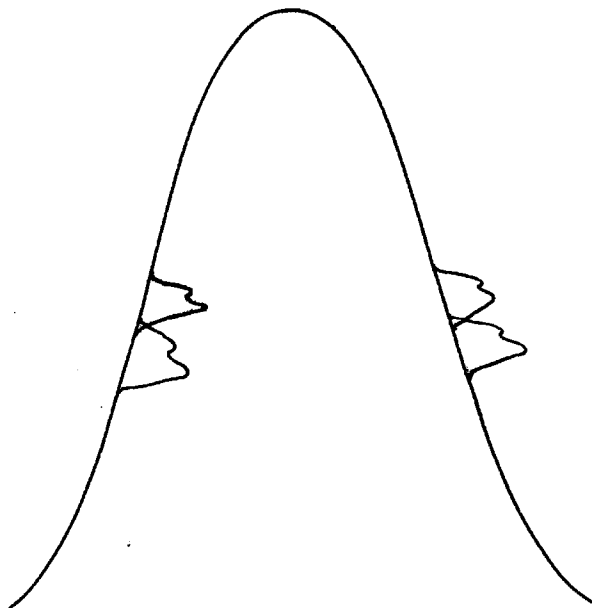


Fig. 6. The Resonance Curve with its Frequency Markers

the receiver. The true position of the frequency marker on the resonance curve can be taken to be the mean position of the two markers. The necessity for taking these effects into account is quite spectacularly demonstrated when the modulation frequency is increased to, say, 50 cycles. At this frequency the pulses are so smeared out that they not only lose the double-hump characteristic of the receiver response but separate and broaden so as to cover a large part of the resonance curve. Fig. 6 also shows the sensitivity of the frequency measurement. Since the markers are only 10 kilocycles wide (or perhaps even 15 kilocycles to allow for some broadening), it is quite possible to set the frequency to, say, 1 kilocycle, since a measurement depends on the horizontal matching of the four pulses. The tolerance on this measurement amounts

to 60 kilocycles, almost two orders of magnitude above the limit of resolution. Further details about other pulses appearing on the resonance curve and the pulses actually used in the measurement, will be found in part IV.

### 3. The Volume Measurement

The simplest method of measuring the cavity volume appeared to be the weighing of the amount of distilled water that can be held by the cavity. It was found that it is not easy to fill the cavity completely with water, but it proved possible.

The method finally adopted is illustrated in Figs. 7 and 8. A glass capillary was sealed into a brass sleeve, using Apiezon wax. A  $41^\circ$  taper, concentric with the brass sleeve, was machine-ground on one end of the capillary tube to match the taper of the iris. The end was faced off by carefully fine-grinding on a piece of polished plate glass, using a jig which assured that the ground surface would be at right angles to the axis of the brass sleeve. This method completely prevented chipping of the edge. Even when looking at the ground surfaces on a "shadowgraph", (magnification  $\sim 100$ ) the edge appeared sharp. The brass sleeve and capillary assembly was fitted into a brass "wing" by means of a split retaining ring, the brass wing in turn being bolted to one of the wave guide flanges of the cavity. A standard ground joint, sealed to the other end of the capillary, was originally intended to connect to the water reservoir; but this connection made the system so rigid that the seal between the cavity and the capillary was too easily disturbed. In the final procedure, the ground joint



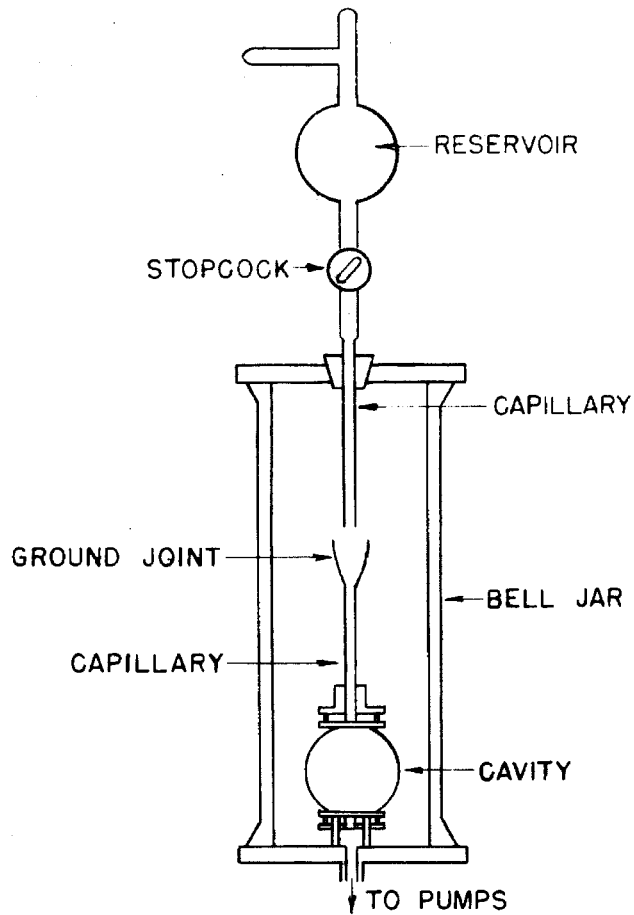


FIG. 7. APPARATUS FOR FILLING CAVITY

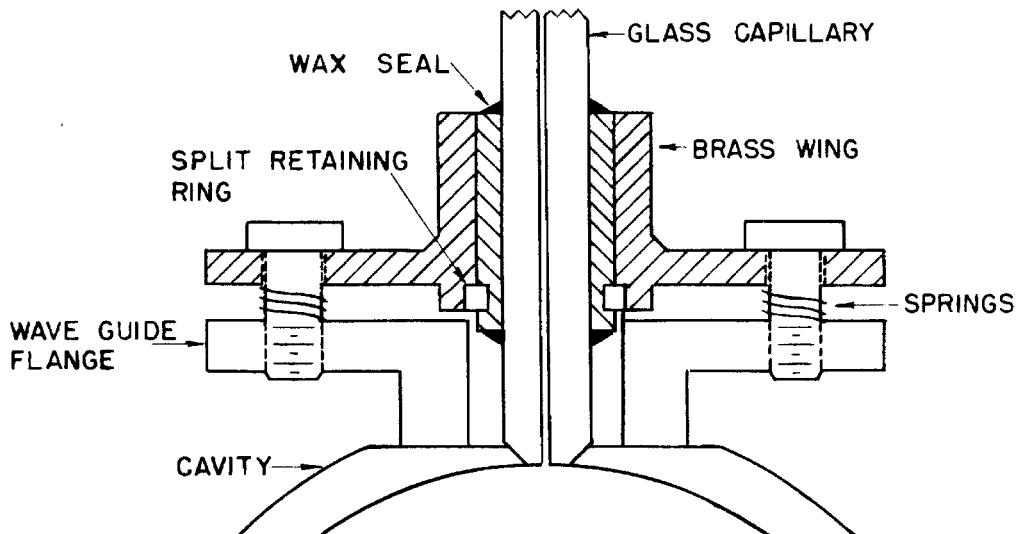


FIG. 8. DETAIL OF JOINT BETWEEN GLASS CAPILLARY AND CAVITY, DOUBLE SCALE

simply served to receive water from another capillary attached to the reservoir, as shown.

A solid brass plug, whose end was also tapered at  $41^{\circ}$ , was bolted to the second wave guide flange, and served to close the other coupling iris. When assembled, with the ends of the capillary and the brass plug protruding one or two thousandths of an inch into the cavity, the actual volume differed from the ideal cylindrical volume by considerably less than the one cubic millimeter tolerance.

The vacuum enclosure consisted of a one foot length of standard Pyrex 4 inch industrial piping, flanged at each end. The grooves in the flanges can be used to make a satisfactory O-ring seal to the brass end plates.

To start the filling process a water aspirator was connected to the water reservoir to pump out most of the dissolved air. The cavity itself was evacuated for some time, before letting water in, a few drops at a time. Enough air would leak into the bell jar system to force the water through the capillary into the cavity. By means of the stop-cock this process could be controlled so that water would not spill over. Eventually the pressure in the cavity would build up to stop the flow of water. The bell jar was then reevacuated and the above process repeated. It was necessary to do this three or four times before "filling" the cavity, the entire procedure taking about 15 minutes. It was not possible to fill the cavity completely in this manner. It took two or three days of alternately pumping with a mechanical forepump and carefully replacing the water pushed out by the escaping air, before the last air bubble could be removed.

To test whether or not the cavity was completely full, the bell jar was alternately evacuated and subjected to atmospheric pressure. The presence of any air bubble at all in the cavity, even if it were much smaller than the allowed one cubic millimeter, would produce an enormous change in level in the capillary. Since water is slightly compressible (compressibility =  $5 \times 10^{-5}$  per atmosphere) there will be some small change in level which can be calculated. For a volume of 60 cubic centimeters this effect amounts to  $5 \times 60 \times 10^{-2}$  cubic millimeters =  $3\text{mm}^3$ . This corresponds to a 2.4 centimeter length in the capillary. The observed level change (in the final volume determination) was about 2 centimeters.

#### 4. The Temperature Measurement

In order to deduce the cavity volume from the measured weight of water it contains, it is necessary to know the density of the water which in turn depends on the temperature. This temperature has to be determined rather accurately. In addition it is necessary to know the temperature of the steel cavity when measuring its resonant frequency. The latter measurement does not, however, require the precision of the former.

The temperature of the water was measured with two thermometers attached to the upper and lower wave guide flanges of the cavity. The thermometer bulb was placed in a short copper cup which was soldered to a parallel type clamp made of copper bars. The clamps were fastened to the wave guide flanges in such a way as not to disturb the brass plug and capillary attachment bolted to the cavity. Tin foil was used

to make good thermal contact between thermometer bulb and cup, and also between clamp and flange.

The cavity, with its two thermometers and the capillary, was set inside a copper cooling coil, and enclosed in the same glass pipe fitting that was used as a vacuum bell jar. Top and bottom of the glass pipe were insulated with one inch thick cork discs. Tap water was run through the cooling coil; this turned out to be an effective, even if somewhat crude, constant-temperature air bath. If necessary, the tap water was run through another copper coil immersed in ice-water. In addition the room was cooled by an air-conditioner set to run at approximately the air bath temperature. Essentially this experiment was a calibration of the cavity and its capillary as a thermometer. Temperature equilibrium was believed to be established after the readings of all three "thermometers" were constant to within a fraction of the tolerance for a period of two hours. (The temperature tolerance in the neighborhood of  $18^{\circ}\text{C}$  is  $\pm 0.05^{\circ}\text{C}$ .)

The same two thermometers were used to read the cavity temperature for the frequency measurement. The thermometers were immersed in oil cups that were bolted to the two wave guide flanges of the cavity. The cups were filled with diffusion pump oil. The two methods of attaching the thermometers to the cavity were thus quite similar and can be relied upon to give the same results under similar circumstances. Actually it would have been better to use the small cups with the tin foil for the frequency measurement also, eliminating the presence of oil vapor in the vacuum system. But the author did not think of the tin foil arrangement until this proved necessary, in connection with the measurement of the water temperature.

#### IV. THE EXPERIMENTS

##### 1. The Frequency Measurement

###### (a) The Frequency Markers

It was mentioned previously that in addition to the rather large primary frequency marker pulses, others were observed on the resonance curve. These pulses are all produced by intermodulation between the various standard signals and the modulated power oscillator signal. The spurious pulses are second, third, or even fourth harmonics. The signal strength of the frequency standards was higher than needed to produce the primary pulses; it was therefore possible, fortunately, to observe these harmonics. The most prominent of these was a pair of markers located half-way between the main pulses and the top of the resonance curve. Let the resonance peak be at  $f_o$ , which is also the setting of the standard. Let the receiver be tuned to  $f_r$ . The receiver responds, therefore, when the power oscillator (2K39) frequency is  $f_o \pm f_r$ . However, at the points defined by  $f_o \pm \frac{1}{2} f_r$ , the mixer crystal produces a second harmonic of the beat frequency  $\frac{1}{2} f_r$ , equal to  $f_r$ , to which the receiver responds also. When the equipment is properly adjusted, a whole series of harmonics can be seen, all the way up to the top of the resonance curve.

It was puzzling to find that the second harmonics were not symmetric with respect to the primary pulses. This effect proved to be due to an asymmetry in the cavity resonance curve itself. The cause of this asymmetry is discussed elsewhere.

Another set of harmonics is schematically reproduced in Fig. 9. This picture is also perplexing at first, since there are an

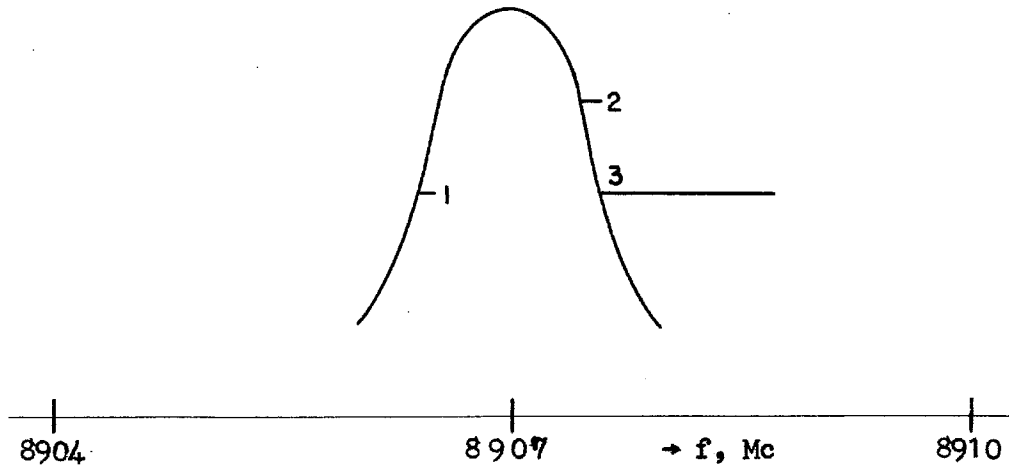


Fig. 9. Resonance Curve with Second Harmonic Frequency Markers.

odd number of pulses. It is obtained when the receiver is approximately tuned to the frequency difference between the fixed standard (8910 megacycles) and the cavity resonance,  $f_0$ . The use of numbers will simplify the following explanation. Let the cavity resonance peak be at  $f_0 = 8907$ . Thus the interpolation oscillator is set to 3 megacycles, and will produce a second harmonic marker at 8904. The main receiver response occurs at  $f_3 = 8910 - f_r$ . There is a second response at  $f_1$ , symmetric with respect to  $f_3$ , given by  $f_1 = 8904 + f_r$ . Another second harmonic marker produced by the crystal is that given by  $8907 + 8910 = 17817 = 2(8908.5)$ . We obtain a receiver response when the second harmonic of  $f_2$  is  $f_r$  below this second harmonic marker, i.e., when  $2f_2 = 2(8908.5) - f_r$  or  $f_2 = 8908.5 - \frac{1}{2} f_r$ . Thus  $f_2$  is exactly

half-way between 8907 ( $f_0$ ) and  $f_3$ , and corresponds to the second harmonic described on page 32. Logically, there should also be a pulse symmetric with respect to  $f_2$ . It is produced by intermodulation between 8904 and 8907. But 8904 is already a second harmonic; so the missing pulse is a second order harmonic, and is too weak to be observed.

The receiver is tuned to about 2 megacycles. At this setting the radio frequency circuits do not limit the bandwidth. In the former method the receiver is tuned to about 150 kilocycles; in this band the response of the radio frequency circuits is too sharp to pass a 10 kilocycle signal properly. The difference showed up in increased distortion and separation of the pulses. For these reasons the method illustrated in Fig. 9 was adopted. The receiver tuning was adjusted so that pulses 1 and 3 were located about half-way between the top of the resonance curve and the half-power points. This is not the most sensitive position, but it was thought advisable to have the markers near the top to reduce as far as possible the effects of the asymmetry of the resonance curve.

It should be pointed out here that the frequency measurement is entirely independent of the receiver calibration. The alignment of 1 and 3 is produced by adjusting the interpolation oscillator to coincidence with  $f_0$ . The frequency of the interpolation oscillator was measured with a BC-221-C frequency meter. The BC-221-C was calibrated twice against a Hewlett-Packard model 525A counter-type frequency meter. The calibrations were performed both before and after the cavity frequency measurement and were within 0.1 kilocycle of each other almost everywhere. The time interval between the two calibrations was over  $1\frac{1}{2}$  years. The BC-221-C readings themselves could be relied on to  $\pm \frac{1}{2}$  kilocycle.

(b) Technique and Precautions

Before each run the cavity was carefully cleaned on the inside as follows:

Rub the surfaces with "Drop Chalk", using distilled water and absorbent surgical cotton.

Clean with acetone and cotton.

Wash in detergent ("Joy") and warm distilled water.

Rinse in warm distilled water.

Dry with clean cotton.

The "Drop Chalk" referred to above turned out to be chemically pure calcium carbonate in finely powdered form. It is used for final cleaning of the surface of the 200 inch Palomar mirror. In the present case it was found ideal because of its extreme softness and its ability to remove tarnish and other foreign matter from the surfaces of the cavity. It produced no scratches whatsoever in the silver. (Silver is much too soft a material for a polishing agent like "rouge" or similar metal oxides.)

In the case of the frequency measurements in vacuo, the diffusion pump was started and allowed to reach minimum pressure ( $10^{-6}$  -  $10^{-5}$  millimeters of mercury). The room was kept as cool as possible with an air-conditioner. The power supply for the 2K39 klystron was adjusted for operation in the highest (power output) mode; the power output was monitored and displayed on an oscilloscope, in order to keep the klystron exactly at the top of the mode. The monitored oscilloscope picture proved to be very sensitive for this purpose.



Only two additional adjustments were necessary to take frequency readings. The 5 megacycle crystal had to be set to, and kept in, coincidence with WWV to the best possible precision; and the interpolation oscillator was adjusted for horizontal alignment of the marker pulses. A measurement, then, consisted of reading the two thermometers and measuring the interpolation oscillator frequency with the BC-221-C. In order to obtain the best possible pulses, the modulation voltage applied to the 2K39 repeller was reduced so as to cover only the top half of the resonance curve, just enough to include the two pulses. This decreased the required bandwidth and thus improved the pulse reproduction. The frequency stability of the power klystron was not always good enough for this purpose, so that some readjustment was occasionally necessary.

(c) Auxiliary Measurements

It was decided fairly early in the experiments to avoid the question of the effect of a wave guide mismatch on the iris correction by matching the 1N23B crystal to the wave guide (the output section). This was done by adjusting two tuning screws and a shorting plunger. The signal level was the same as that used in the frequency measurement. A voltage standing wave ratio of 1.03 was obtained, using a "Millivac" to measure the d-c crystal output.\* This ratio was constant over a frequency range of  $\pm 5$  megacycles and centered around 8904 megacycles. The input wave guide should similarly have been matched. This was postponed at the time because the author was not sure that the resultant

---

\* The "Millivac" is a chopper-type d-c millivoltmeter.

unbalance of the magic T would be of no consequence. Later on there was not time to correct this remaining mismatch.

It was desired to measure the  $Q$  of the cavity. For this purpose the 1N23B crystal had to be calibrated. This was done in the standard way by measuring the electric field in a slotted wave guide shorted at one end.

In the experimental set-up, microwave power was supplied to the crystal through the same detector section as used in the frequency measurement, the connection to the slotted section being made by a coax-to-wave guide adapter and a coaxial line. Measurements were taken with a "Millivac" which was carefully calibrated. The "Millivac" was used so that the signal level could be reduced to that used in the frequency measurement. The exponent of the crystal law was found to lie between 2.0 and 2.1. Thus, for the purposes of the  $Q$  measurement the points on the oscilloscope screen at which the response was half the maximum value could be used as the "half-power" points defining bandwidth and  $Q$ . In the measurement the pulses were adjusted so that the half-power points were half-way between corresponding peaks of the two adjacent pulses; i.e. the two large peaks (see Fig. 6). The bandwidth was determined by multiplying the receiver setting by 2. The receiver was calibrated at the large peak of its response curve.

Measurements were also made of the cavity resonance frequency in air, as a function of cavity temperature. The humidity of the air was measured by a "sling-psychrometer"; the pressure was estimated by reading a barometer in a different building, and correcting for the difference in elevation. From these measurements the corresponding

resonant frequencies in vacuum were calculated, using the latest available formula for the refractive index of air. This formula is (8)

$$N = (n - 1) 10^6 = \frac{103.5}{T} (p + 4810 \frac{e}{T}) \quad (4.1)$$

where

n = refractive index of air

p = total pressure in mm Hg

e = water vapor pressure in mm Hg

T = air temperature in degrees Kelvin.

## 2. The Volume Measurement

One of the worst difficulties encountered in this measurement was the sealing of the cavity with its attachments. It turned out that the cylinder body and end plate surfaces were not quite flat enough to prevent water leakage when assembled dry. If there had been time to make a new cavity and repeat the frequency measurements, this fault would have been corrected, since it is relatively easy to produce flat surfaces that are water-tight when bolted together. For one measurement a thin lacquer was applied from the outside, but it did not penetrate far enough into the dead space to prevent water from getting into the bolt-holes. For this reason an excess volume was measured. For the second measurement it was decided to use regular stopcock grease (A.H. Thomas "Lubriseal"). One of the cavity end surfaces was greased fairly heavily and warmed up under a heating lamp, before the end plates were bolted to it. Excess grease was then carefully removed with cotton and a small amount of acetone.

The other end surface was greased sparingly, heated and closed up as before. Grease was also applied to the seals at the two irises.

When attaching the capillary and brass plug to the cavity care was taken, 1) not to make the connection too tight, and, 2) to keep the brass wings parallel to the wave guide flange of the cavity, in order to effect proper seating of the taper joint.

The capillary was carefully cleaned as follows:

Soak with "glass cleaning solution" (sulphuric acid and potassium permanganate).

Rinse with tap water.

Soak with concentrated nitric acid.

Rinse with tap water.

Soak with ethyl alcohol.

Rinse with tap water.

Rinse with distilled water.

After the cavity was made ready for filling with water, it was first weighed, empty. It was then filled with water as far as possible, following the procedure already described. The removal of the last air bubble from the cavity turned out to be a tedious and long procedure. One source of this difficulty was the use of stopcock grease. It was found later that "Lubriseal" has many volatile components and perhaps a large amount of absorbed air. All these gases had to be pumped out of the grease, most of which was between the cavity body and the end plates.

The following procedure, when repeated often enough, finally led to success. With about  $\frac{1}{2}$  inch of water in the ground joint at the top of the capillary let the aspirator pump on the bell jar system for about 10 minutes. Then connect the forepump to the bell jar (through a dry ice-acetone freezing trap), and carefully adjust the stopcock so that the pump removes air at a relatively low rate, for about 10 minutes. It is possible to do this without freezing the water. In letting the air bubble through the  $\frac{1}{2}$  inch of water some loss of water cannot be avoided. This water is replaced by letting in fresh water from the top. It is important never to expose the inside of the cavity to any air in this process. Thus it is important to have enough water in the ground joint, so that, when at the end of this procedure air is let into the bell jar the water level will not drop below the top of the capillary.

After the cavity was filled, and calibrated as a thermometer, it was stoppered to prevent loss of water, the glass stopper having been made to fit the ground joint. It was then taken to the precision balance to be weighed. At this point it should be made clear that once the temperature measurement is made, the cavity and water temperature is no longer of importance at the weighing except as it affects the air buoyancy correction.

The water used for these measurements was commercial distilled water obtained from Arrowhead and Puritas Waters, Inc. (Los Angeles, California). The purity of this product is higher than that of the "conductivity water" that the California Institute's Chemistry Department made, until recently, from its regular distilled water by triple

distillation. Conductivity measurements yield impurities (sodium chloride equivalent) of the order of 1 part per million, while chemical analysis arrives at about 0.1 milligram per 50 grams. The tolerance in the present experiment is 1 milligram per 50 grams.

(a) Auxiliary Measurements

The capillary was calibrated by weighing it filled with distilled water columns of varying lengths. An analytical balance was used for this purpose. The first weighing was made with the maximum amount of water. Water was then successively removed by putting the capillary in a bell jar and evacuating the system with a water aspirator. If water were removed some other way, some water might cling to the unfilled part of the capillary.

It turned out that when bolting the second end plate to the cavity (see page 39) some grease was forced out of the interstice and formed a small fillet on the inside of the cavity. To estimate the volume this fillet occupied, the grease was weighed, and its density was measured. To weigh the grease, the cavity was emptied, the attachments and the first plate removed, and the remainder was carefully dried. A weighing was then made, the grease fillet removed with cotton and acetone, as before, and a second weighing was made. To determine the density, grease immersed in water was subjected to an aspirator vacuum until gas bubbles stopped developing. A series of four weighings, two in water, two in air, were then necessary to determine weight and volume of the grease sample. The water temperature was approximately that of the main volume measurement.

Indicator measurements were made to determine how far the glass capillary and the brass plug protruded into the cavity. A  $\frac{1}{10,000}$  inch indicator was used in such a way as to measure the difference between the cylindrical surface and the center of the plugs. It was possible, after disassembling and reassembling, to repeat these measurements to about  $\frac{2}{10,000}$  inch.

Finally, the cavity diameter and the length were measured with micrometers to determine whether  $\rho = \frac{L}{D}$  was actually within the tolerance, and also to determine the variation in L and in D. The latter is necessary to calculate the possible error due to grooves.

### 3. The Weighings

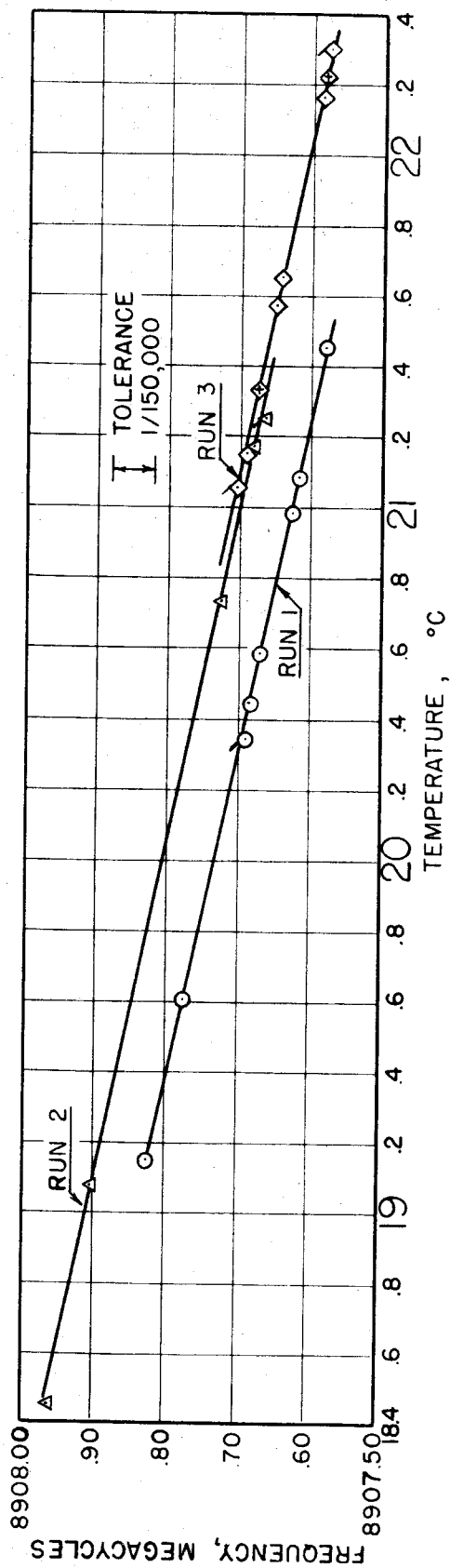
The cavity was weighed on a precision balance, whose capacity is 2 kilograms. (The balance was kindly made available to the author by the Chemical Engineering Department at the California Institute.) The resolution of the weighings was about  $\frac{1}{2}$  milligram. The substitution method was used throughout. A tare weight was made of cold-rolled steel to match the material of the cavity. An attempt was made approximately to equalize surface areas on both sides. Weighings were made, then, by replacing the weight of the water with balance weights on the left hand pan (i.e. the pan holding the cavity). This method not only eliminates any possible errors due to a small difference in lever arms, but it also has the desirable feature that all weighings are made with exactly the same loading of the balance. In making a number of weighings the author became familiar with the effects of small shifts in the balance

point not only during a weighing, but those due to loading of the balance. Since the same procedure was followed for both the "empty" and the "full" weighings, errors due to such shifts are believed nearly to cancel, at least when a tolerance of 1 milligram is given. The balance point was established by noting three swings, always ignoring the very first one. The balance point was then computed as the mean of these swings, giving the middle one a weight of 2. Balance point readings were taken until at least two agreed within 0.2 division. It happens occasionally that the main knife edge does not come to rest properly, causing a "wrong" reading. After each weighing, barometer and temperature readings were taken right next to the balance case; humidity was also measured near the balance, using the "sling-psychrometer".

#### 4. Experimental Results.

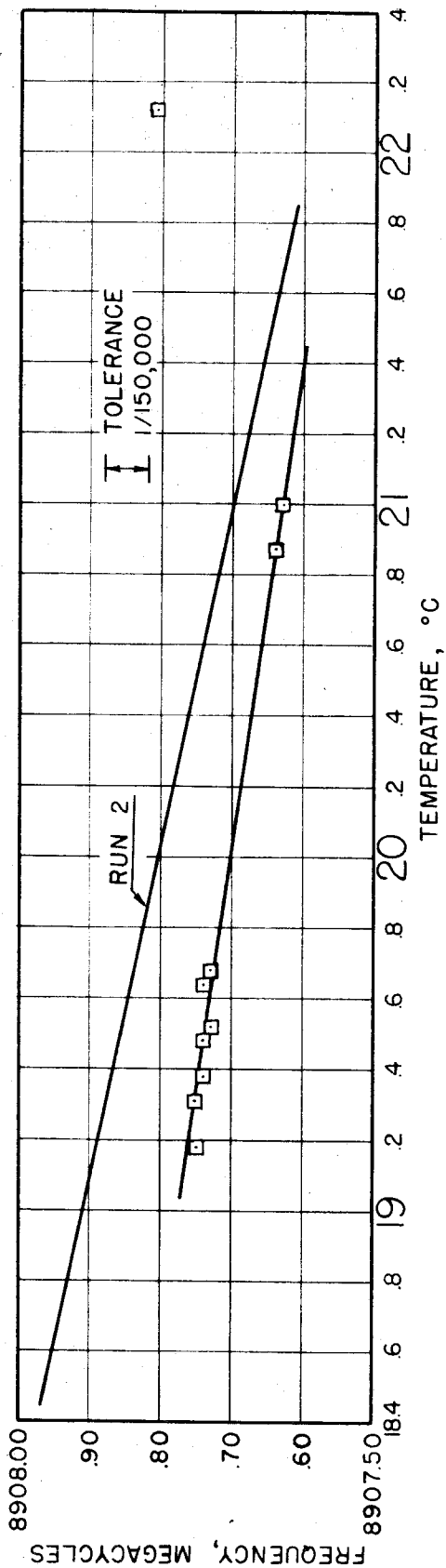
The results of the measurements of resonant frequency, in vacuo and in air, as a function of temperature, are shown in Figs. 10 and 11. The data of Run 1 lie on a straight line, with a maximum deviation, by calculation, of 1 part in 5,000,000. From the slope of this line the linear coefficient of thermal expansion of cold-rolled steel can be calculated. The slope is 105.4 kilocycles per degree centigrade. Thus  $\alpha = \left| \frac{df}{f_0} \right| = \frac{0.1054}{8908} = 1.18 \times 10^{-5}$  per °C. This lies within the range of values given in the Metals Handbook (9):  $1.17 \times 10^{-5}$  per °C to  $1.25 \times 10^{-5}$  per °C for No. 1020 SAE steel. In fact the argument can be turned around: the frequency measurements are so good, even when small differences are considered, that they can





- RUN 1, at reduced power
  - △ RUN 2, at reduced power
  - ◇ RUN 3, "good" readings
  - ◇ RUN 3, temperature differential: 0.31-0.38°C
- 9/21/53 - 10/9/53

FIGURE 10- MEASURED CAVITY RESONANCE FREQUENCY IN VACUO  
VS.  
TEMPERATURE



NOTE: RUN 2, from Figure 10, shown for comparison

7/24/53 - 8/13/53

FIGURE 11-CAVITY RESONANCE FREQUENCY IN VACUO CALCULATED FROM MEASUREMENTS IN AIR  
VS.  
TEMPERATURE

be used to determine coefficients of expansion of a particular sample for very small temperature ranges. The results are better than those obtained from handbooks.

The cavity was disassembled, cleaned, and reassembled between runs, this process causing some shift in the resonance frequency. It appears that in assembling the cavity for Run 1 a small amount of foreign matter was left on the flat surfaces, increasing the volume and decreasing the frequency. When assembling the cavity for Run 3 especial care was taken to remove all lint from the surfaces to be bolted together. This was very nearly accomplished, for the shift in resonant frequency between Runs 2 and 3 amounts to only 1 part in 1,000,000.

In order to discover experimentally the effect of a wave guide mismatch on the resonant frequency, the setting of the attenuator near the 2K39 power klystron was changed so as to reduce the power level by a factor of 10. This produced a small ( $1 \text{ part in } 10^6$ ) but noticeable drop in the resonant frequency, as shown by the points marked "reduced power". It was found later that the attenuator setting had very little effect on the standing-wave ratio as seen from the cavity. This means that there is not sufficient evidence that the wave guide mismatch can be neglected. However, the information is useful for qualitative estimates.

There are two points in Run 3 that were taken when the readings of the two thermometers differed by almost  $0.4^{\circ}\text{C}$ . For most of the other measurements the thermometers agreed to better than  $0.1^{\circ}\text{C}$ .

## 5. Calculations

The complete calculations, using the last volume measurement, are shown below.

### Volume Measurement

#### Data:

#### I. Weighing of cavity, empty:

Weights added: 79.5667 g

Barometer reading: 741.0 mm Hg

Temperature: 22.5 °C

Psychrometer readings: 70 °F/61.4 °F

#### II. Weighing of cavity, full:

Weights added: 21.8737 g

Barometer reading: 745.3 mm Hg

Temperature: 22.4 °C

Psychrometer readings: 69.2 °F/59.8 °F

### Calculation of Air Buoyancy:

#### Weighing I

Barometer correction (for altitude, latitude, and temperature): -3.5 mm Hg

Corrected pressure: 737.5 mm Hg

From psychrometer readings, water vapor pressure: 11.58 mm Hg

Density of air: 1.1523 mg/ml = 1.1523 mg/cm<sup>3</sup>

## Weighing II

Barometer correction: -3.5 mm Hg

Corrected pressure: 741.8 mm Hg

Water vapor pressure: 10.28 mm Hg

Density of air: 1.1601 mg/cm<sup>3</sup>

## Calculation of Volume:

Net measured weight of water: 57.6930 g

Buoyancy correction for stainless steel weights of  
density 7.7, a representative value:

$$- 57.69 \times \frac{1.152}{7.7} \times 10^{-3} = - 0.0086 \text{ g}$$

Buoyancy correction for water:

$$+ 57.69 \times 1.160/0.998 \text{ mg} = + 0.0671 \text{ g}$$

True weight of water: 57.7515 g

Total volume (density = 0.998741 g/cm<sup>3</sup>\* at 17.20 °C): 57.8243 cm<sup>3</sup>

Excess volume in capillary:

Length of water column: 6.75 cm.

From capillary calibration of 0.800 cm per mm<sup>3</sup>,

Volume correction: - 0.0084 cm<sup>3</sup>

Correction for grease fillet

Weight of grease: 16.0

Density of grease: 0.84 g/cm<sup>3</sup>

Volume correction: + 0.0190 cm<sup>3</sup>

---

\* The Handbook (10) gives 0.998739 g/cm<sup>3</sup>. However, Glazebrook (11) whose table was checked against the original calibration of the liter (12), shows the value 0.998741 g/cm<sup>3</sup>.

Net volume correction due to protrusion of capillary and  
plug

$$+ 0.0001 \text{ cm}^3$$

True cavity volume at 17.20 °C:

$$57.8350 \text{ cm}^3$$

### Frequency Measurement

Resonant frequency, in vacuo, at 17.20 °C, extrapolated: 8908.10 Mc

Iris correction:

$$A_1 \pi \frac{4}{3} \frac{M}{V} f_0 \quad (\text{see pp. 12, 18}), \text{ using } A_1 = 0.224,$$

$$M = \frac{4}{3} c^3, \quad c = 0.179 \text{ cm:} \quad + 1.10 \text{ Mc}$$

Correction due to finite conductivity of walls:

$$\Delta f = \frac{1}{2} \text{ bandwidth} = \frac{1}{2} \times 0.32 \text{ Mc} = + 0.16 \text{ Mc}$$

Second order correction due to mismatch of input wave guide,

$$(\text{estimated, see part V}): \quad - 0.02 \text{ Mc}$$

Ideal resonance frequency, in vacuo, at 17.20 °C:

$$8909.34 \text{ Mc}$$

### The Velocity of Light

From (2.4)

$$c = \frac{f}{\sqrt{3}} \times \sqrt[3]{\frac{16\pi V}{(kR)^2}}$$

Substituting  $(kR) = 3.8317060$ , (2.4) becomes

$$c = 0.8701642 f \sqrt[3]{V}$$

For  $f = 8909.34$  megacycles, and  $V = 57.8350$  cubic centimeters

$$c = 299,809 \text{ km/sec.}$$

## 6. Calibrations

The thermometers were calibrated against a National Bureau of Standards certified thermometer. The three thermometers were immersed in a commercial temperature-controlled water bath in such a way that the scale readings at the water - air interface were identical. This was done to eliminate completely any small stem correction. The thermometers were kept in the water bath for one hour; the temperature rose gradually a total amount of  $0.2^{\circ}\text{C}$ . The air temperature varied a total of about  $0.15^{\circ}\text{C}$ . The last set of readings was used for the calibration.

The balance weights were calibrated against a 1 gram and a 10 gram standard, both of which are also certified by the National Bureau of Standards. The substitution method was used again. The weighings were done on a "Chainomatic" analytical balance; they were arranged so that always the same portion of the chain was used: all readings were between 9.30 and 10.17 milligrams. In the calculations the density of the standards (brass) was taken as 8.3 grams per cubic centimeter; the stainless steel weights were assumed to have a density of 7.7 grams per cubic centimeter. The results were in substantial agreement with previous calibrations of the same set of weights. In fact the author's calibration and that used by the Chemical Engineering Department resulted in precisely the same answer for the net weight of water contained in the cavity.

## V. DISCUSSION

### 1. The interfering $TM_{111}$ mode

The author became aware of the existence of a second resonant mode in the cavity when reading an article by K. Shimoda (13) on mode coupling due to tilted end plates. The difficulty arises because the cut-off parameter of the  $TM_{11}$  wave guide mode is determined by  $J_1(kR) = 0$ , which also defines the cut-off parameter of the  $TE_{01}$  mode, given by  $J'_0(kR) = 0$ , since  $J_1(x_0) = 0 = J'_0(x_0)$ . The problem is a fundamental one: for all TE modes possessing the very desirable property of having no wall currents cross the joints between the three parts of the cavity, there are TM modes resonating at the "same" frequency. One approach, then, would be to sacrifice this one good feature, and use a mode other than  $TE_{0np}$ . In that case the end surfaces would have to be very flat and clean. This can be done, and it is possible to obtain Q's approaching theoretical values, even for these modes. According to a recent survey article (14), K. Bol (4) inserted a gap between the cylindrical body and each end plate of the cavity to suppress undesired modes. This is another approach, but it may prove difficult to correct for the effect of the gaps.

In the present experiment the excitation of the  $TM_{111}$  mode is very low compared to that of the  $TE_{011}$  mode, because the magnetic field of the TM mode has a zero at the center of the iris. The Q of the TM mode is considerably lower than that of the TE mode. This has two effects: 1) the TM resonance frequency will be lower than that of the TE mode; 2) the shift in the exact position of the



true peak of the resonance curve should be very small. It may be possible to calculate the exact shape of the resonance curve, taking into account not only the excitation at the irises, but the coupling due to losses at the walls and deformation of the cavity surface. Off-hand, it would seem that the presence of the TM mode would lower the resonance frequency. This correction would increase the calculated value of the velocity of light, and would thus not explain the 16 km/sec excess (compared to Bergstrand's value) obtained in these experiments. However, the direction of the shift in resonance frequency may depend on the phase relationship between the two modes. Experimentally the asymmetry was found to be less than 30 kilocycles, half the tolerance. By the "asymmetry" is meant the frequency difference between the mean of the "half-power" points and that of the "three-quarter" power points. This evidence indicates that the frequency shift due to mode coupling may be quite negligible, if the frequency markers are located near the top of the resonance curve.

## 2. The input wave guide mismatch

From some crude measurements the voltage standing wave ratios were obtained as follows: 6.5 for the normal attenuation setting; 2.8 for the "Reduced Power" setting (see p.46). The positions of the maxima and minima were the same for both settings. The maximum susceptance corresponding to a VSWR of 6.5 is  $b_T = 3$ , and, if inductive, would decrease the iris correction,  $\Delta f_0$ , by  $(0.008 \times 3)\Delta f_0 = 15$  kilocycles, using (2.32). The corresponding susceptance for a voltage

standing wave ratio of 2.8 is  $b_T = 1$ , causing a shift of 5 kilocycles. The difference, 10 kilocycles, was actually observed (see Fig. 10); but this should not be taken as a numerical check, since the admittance measurements were both crude and incomplete. In order to account for the measured excess of 16 km/sec almost the entire iris correction would have to be cancelled. This would require near resonance of, and very low losses in, the input wave guide section, as in Case 2, p. 16. Such a condition is possible but not likely. It is for this reason that the ABSTRACT lists a minimum value rather than a probable error.

### 3. Additional Sources of Error

In order to determine the iris correction itself, the values of  $A_1$  and  $M$  have to be known. Gruenberg (5, p. 47) calculates  $A_1$  for irises with taper angles  $90^\circ$ ,  $45^\circ$ , and  $0^\circ$ . Adding  $A_1 = 0$  for a taper angle of  $-90^\circ$  and plotting these four points one can estimate the value of  $A_1$  corresponding to a taper of  $41^\circ$ , the actual angle of the tapered iris. A small additional correction is allowed for the short section of the iris hole which is not tapered. (See Fig. 12) The hole diameter was measured with a microscope comparator in order to calculate the value of  $M$ . Maximum variations were  $\pm 0.001$  centimeters, representing an uncertainty of 10 kilocycles, or one-sixth of the tolerance.

The bandwidth of the resonance curve was measured; it was found to be 399 kilocycles at the normal power level, 357 kilocycles

at "reduced power". The value 0.32 megacycle was used in the calculations on p. 49 to allow for 1) the effect of the mismatch, as in section 2, and 2) the power radiated from the irises in the matched case, which decreases the  $Q$  by 1.04 (see Gruenberg (5), p. 42).

In order to estimate the effect of grooves in the cavity surface, assume grooves of depth 0.001 inch and width 0.002 inch. Using both (2.19) and (2.20) the total error would be  $< 2 \times 10^{-6}$  corresponding to about  $\frac{1}{2}$  km/sec. The probable error due to this cause is much less than  $\frac{1}{2}$  km/sec, however, since the grooves will be randomly distributed and their effects will tend to cancel, as pointed out by Gruenberg (5, p. 38). Formulas (2.19) and (2.20) were calculated for grooves located in regions where the magnetic field is a maximum. For grooves in regions where the electric field predominates, the frequency shift has the opposite sign.

Fig. 12 shows the joint between the cavity and the capillary in detail. The shaded areas represent excess or defect in volume compared to that defined by the ideal cavity surface. The brass plug joint is similar except that the plug protrudes into the cavity an additional 0.002 inch. The net volume difference is calculated to be + 0.0001 cubic centimeter. (This was accomplished by first developing an accurate formula for the intersection of a cylinder and a cone.) Shadowgraph measurements of the end diameters of capillary and plug were consistent with the respective indicator measurements of the protrusions into the cavity, after allowing 0.0085 inch for the straight portion of the iris.

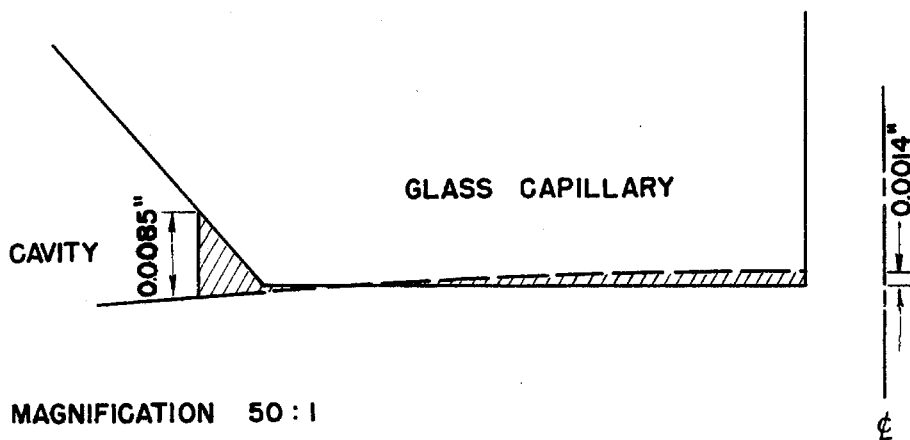


Fig. 12. Enlarged Detail of Iris and Capillary.

Another error might be caused by bulging of the end plates due to hydrostatic pressure when the cavity is filled with water. Using the pressure at the very bottom of the cavity and applying it uniformly to the surface at the end plates, the increase in volume is calculated to be  $< 0.01$  cubic millimeter, which is completely negligible.

In order to eliminate any errors due to distortion caused by the weight of the cavity itself, the cavity was always supported from the "bottom" flange during the temperature - volume measurements as well as the frequency measurements.

The author feels sure that the measured quantities themselves are well within the tolerance of 1 part in 150,000. This is shown for the frequency measurement by Fig. 10. Unfortunately there was not time to repeat the volume measurement, (no. 2), on which the calculations were based. The result of this measurement was about 30 cubic millimeters below that of measurement no. 1. In the case of measurement no. 1 the cavity was only sealed from the outside. The difference

can reasonably be ascribed to the volume between the contact surfaces and the clearance space in the bolt-holes. The former, as calculated from indicator measurements, accounts for about 10 cubic millimeters; the remaining 20 cubic millimeters being a possible value for the latter.

#### 4. The Dielectric Constant of Air

Fig. 11 shows that it is difficult to make psychrometer measurements that are accurate enough for a precise determination of the dielectric constant of air. The results indicate an error in the refractive index of about 3 per cent. The point corresponding to a temperature of about 22.1 °C was the very first measurement, in which the psychrometer was used improperly. It is therefore not surprising to find an abnormally large error in this measurement.

If the purpose of this part of the experiment was to obtain an approximate check on the dielectric constant of air, it can be judged that the project was successful. In order to attain higher precision, controlled samples of air must be introduced into an evacuated cavity whose surfaces have been carefully freed from all absorbed moisture.

A look at the formula for the refractive index of air (4.1) shows that for the measurements in vacuo a total pressure of  $10^{-3}$  millimeters of mercury is conservative when a tolerance of 1 part in 150,000 is considered. The diffusion pump actually produced pressures ranging from  $2 \times 10^{-6}$  mm Hg to  $4 \times 10^{-5}$  mm Hg. There was no measurable frequency shift in this range of pressures.

## 5. Conclusions

It must be concluded that the method employed in this measurement of the speed of light is not only good in principle, but feasible in practice. The principal experimental difficulty in the measurement of the volume was overcome, 1) by use of a high capacity precision balance, and, 2) by the application of the compressibility test (see p. 30). In considering any further work on this particular method the following improvements suggest themselves:

(a) The surfaces of the cavity body and end plates should be made flat enough to make the joints water-tight without the use of any grease.

(b) Some thought should be given to a design of the iris holes to allow a simplification of the capillary and plug attachments. If, in addition, the iris radius were decreased by a factor of 1.5, the iris correction would be decreased to 325 kilocycles, only  $5\frac{1}{2}$  times the tolerance. The transmitted power would be reduced by a factor of 10, at which level frequency measurements are still easily made, as shown by the "Reduced Power" experiments.

(c) The input wave guide should be matched, or, if not, proper measurements should be made in conjunction with the theory of pp. 16 - 18.

The result obtained by the author at least confirms the recent evidence that the value adopted by Birge in 1941 is too low by an amount considerably in excess of the quoted probable error. If no large systematic error is found in the present work, even Bergstrand's value (299,793 km/sec) is probably somewhat too low.

APPENDIX

Principal Symbols Used

The rationalized M.K.S. system is used throughout.

Vectors are indicated by a bar underneath the letter, and complex numbers and their conjugate by the symbols ( $\vee$ ) and ( $\wedge$ ) above the letter.

|  |  |
|--|--|
| $\underline{A}$  | magnetic vector potential                                  |
| $\underline{A}^{\circ}$                                | normalized vector potential                                |
| $A_1$  | coefficient of iris polarizability                         |
| $a$  | subscript referring to the $a$ th cavity mode              |
| $a$  | wide dimension of wave guides                              |
| $\underline{a}_r, \underline{a}_\phi, \underline{a}_z$ | unit vectors in cylindrical coordinates                    |
| $\underline{B}$  | magnetic induction   |
| $\underline{B}^{\circ}$                                | normalized magnetic field                                  |
| $\underline{B}_0$                                      | magnetic exciting field at iris                            |
| $\underline{B}(0)$                                     | magnetic field at center of iris                           |
| $\underline{B}_w$                                      | magnetic field in the wave guide, $TE_{10}$ mode component |
| $b$  | narrow dimension of wave guides                            |
| $b_T$  | wave guide susceptance                                     |
| $c$  | velocity of light  |
| $c$  | radius of coupling irises                                  |
| $D$  | diameter of cavity   |
| $\underline{E}$  | electric field intensity                                   |
| $\underline{E}^{\circ}$                                | normalized electric field                                  |

|                 |   |
|-----------------|---|
| $f$             | resonance frequency of cavity                               |
| $\check{f}$     | iris correction factor                                      |
| $g_T$           | wave guide conductance                                      |
| $j$             | square root of -1   |
| $k$             | cut-off phase constant for $TE_{01}$ mode in circular guide |
| $K_T$           | wave guide reflection coefficient                           |
| $L$             | length of cavity  |
| $M$             | magnetic polarizability of iris                             |
| $\underline{n}$ | unit vector normal to cavity surface                        |
| $p_a$           | amplitude of a th cavity mode                               |
| $R$             | radius of cavity  |
| $R_s$           | skin-effect surface resistance                              |
| $S$             | surface of cavity   |
| $V$             | cavity volume   |
| $y_T$           | wave guide admittance                                       |
| $\beta$         | wave number $\frac{2\pi f}{c}$                              |
| $\lambda_g$     | guide wave length   |
| $\rho$          | length-to-diameter ratio of cavity                          |
| $\rho$          | radius variable in the iris at the cavity surface           |
| $\Psi$          | ratio of cavity and matched wave guide fields               |
| $\omega$        | angular frequency   |



# REFERENCES

- (1) Michelson, A.A., Astrophysical Journal, 65 (1927), 1.
- (2) Birge, R.T., Reviews of Modern Physics, 13 (1941), 233.
- (3) Bergstrand, E., Arkiv för Fysik, 3 (1951), 479.
- (4) Bol, K., Physical Review, 80 (1950), 298.
- (5) Gruenberg, H., Doctorate Thesis, California Institute of Technology (1949).
- (6) Smythe, W.R., Static and Dynamic Electricity, 1950, second edition, New York, McGraw-Hill.
- (7) Smythe, W.R., Physical Review, 72 (1947), 1066.
- (8) Smith, E.K. and Weintraub, S., National Bureau of Standards, Report No. 1938, September 19, 1952.
- (9) The American Society for Metals, Metals Handbook, 1948, p. 309; 1939, pp. 486-487.
- (10) Hodgman, C.D., Handbook of Chemistry and Physics, 31st edition, 1949, Cleveland, Chemical Rubber Publishing Co., p. 1720.
- (11) Glazebrook, Sir R., A Dictionary of Applied Physics, vol. III, 1923, MacMillan and Co. Ltd., London, pp. 130,776.
- (12) Bureau International des poids et mesures, Travaux et Mémoires, t. XIII (1907), p. D40, and t. XIV (1910).
- (13) Shimoda, K., Journal of the Physical Society of Japan, 6, No. 5, September/October 1951.
- (14) Mulligan, J.F., American Journal of Physics, 20, (1952), 165.